

Measurement of charged particle multiplicities in gluon and quark jets in $p\bar{p}$ collisions at $\sqrt{s} = 1.8$ TeV

D. Acosta,¹⁴ T. Affolder,⁷ M.G. Albrow,¹³ D. Ambrose,³⁶ D. Amidei,²⁷ K. Anikeev,²⁶ J. Antos,¹ G. Apollinari,¹³ T. Arisawa,⁵⁰ A. Artikov,¹¹ W. Ashmanskas,² F. Azfar,³⁴ P. Azzi-Bacchetta,³⁵ N. Bacchetta,³⁵ H. Bachacou,²⁴ W. Badgett,¹³ A. Barbaro-Galtieri,²⁴ V.E. Barnes,³⁹ B.A. Barnett,²¹ S. Baroiant,⁵ M. Barone,¹⁵ G. Bauer,²⁶ F. Bedeschi,³⁷ S. Behari,²¹ S. Belforte,⁴⁷ W.H. Bell,¹⁷ G. Bellettini,³⁷ J. Bellinger,⁵¹ D. Benjamin,¹² A. Beretvas,¹³ A. Bhatti,⁴¹ M. Binkley,¹³ D. Bisello,³⁵ M. Bishai,¹³ R.E. Blair,² C. Blocker,⁴ K. Bloom,²⁷ B. Blumenfeld,²¹ A. Bocci,⁴¹ A. Bodek,⁴⁰ G. Bolla,³⁹ A. Bolshov,²⁶ D. Bortoletto,³⁹ J. Boudreau,³⁸ C. Bromberg,²⁸ E. Brubaker,²⁴ J. Budagov,¹¹ H.S. Budd,⁴⁰ K. Burkett,¹³ G. Busetto,³⁵ K.L. Byrum,² S. Cabrera,¹² M. Campbell,²⁷ W. Carithers,²⁴ D. Carlsmith,⁵¹ A. Castro,³ D. Cauz,⁴⁷ A. Cerri,²⁴ L. Cerrito,²⁰ J. Chapman,²⁷ C. Chen,³⁶ Y.C. Chen,¹ M. Chertok,⁵ G. Chiarelli,³⁷ G. Chlachidze,¹³ F. Chlebana,¹³ M.L. Chu,¹ J.Y. Chung,³² W.-H. Chung,⁵¹ Y.S. Chung,⁴⁰ C.I. Ciobanu,²⁰ A.G. Clark,¹⁶ M. Coca,⁴⁰ A. Connolly,²⁴ M. Convery,⁴¹ J. Conway,⁴³ M. Cordelli,¹⁵ J. Cranshaw,⁴⁵ R. Culbertson,¹³ D. Dagenhart,⁴ S. D'Auria,¹⁷ P. de Barbaro,⁴⁰ S. De Cecco,⁴² S. Dell'Agnello,¹⁵ M. Dell'Orso,³⁷ S. Demers,⁴⁰ L. Demortier,⁴¹ M. Deninno,³ D. De Pedis,⁴² P.F. Derwent,¹³ C. Dionisi,⁴² J.R. Dittmann,¹³ A. Dominguez,²⁴ S. Donati,³⁷ M. D'Onofrio,¹⁶ T. Dorigo,³⁵ N. Eddy,²⁰ R. Erbacher,¹³ D. Errede,²⁰ S. Errede,²⁰ R. Eusebi,⁴⁰ S. Farrington,¹⁷ R.G. Feild,⁵² J.P. Fernandez,³⁹ C. Ferretti,²⁷ R.D. Field,¹⁴ I. Fiori,³⁷ B. Flaughner,¹³ L.R. Flores-Castillo,³⁸ G.W. Foster,¹³ M. Franklin,¹⁸ J. Friedman,²⁶ I. Furic,²⁶ M. Gallinaro,⁴¹ M. Garcia-Sciveres,²⁴ A.F. Garfinkel,³⁹ C. Gay,⁵² D.W. Gerdes,²⁷ E. Gerstein,⁹ S. Giagu,⁴² P. Giannetti,³⁷ K. Giolo,³⁹ M. Giordani,⁴⁷ P. Giromini,¹⁵ V. Glagolev,¹¹ D. Glenzinski,¹³ M. Gold,³⁰ N. Goldschmidt,²⁷ J. Goldstein,³⁴ G. Gomez,⁸ M. Goncharov,⁴⁴ I. Gorelov,³⁰ A.T. Goshaw,¹² Y. Gotra,³⁸ K. Goulianos,⁴¹ A. Gresele,³ C. Grosso-Pilcher,¹⁰ M. Guenther,³⁹ J. Guimaraes da Costa,¹⁸ C. Haber,²⁴ S.R. Hahn,¹³ E. Halkiadakis,⁴⁰ R. Handler,⁵¹ F. Happacher,¹⁵ K. Hara,⁴⁸ R.M. Harris,¹³ F. Hartmann,²² K. Hatakeyama,⁴¹ J. Hauser,⁶ J. Heinrich,³⁶ M. Hennecke,²² M. Herndon,²¹ C. Hill,⁷ A. Hocker,⁴⁰ K.D. Hoffman,¹⁰ S. Hou,¹ B.T. Huffman,³⁴ R. Hughes,³² J. Huston,²⁸ C. Issever,⁷ J. Incandela,⁷ G. Introzzi,³⁷ M. Iori,⁴² A. Ivanov,⁴⁰ Y. Iwata,¹⁹ B. Iyutin,²⁶ E. James,¹³ M. Jones,³⁹ T. Kamon,⁴⁴ J. Kang,²⁷ M. Karagoz Unel,³¹ S. Kartal,¹³ H. Kasha,⁵² Y. Kato,³³ R.D. Kennedy,¹³ R. Kephart,¹³ B. Kilminster,⁴⁰ D.H. Kim,²³ H.S. Kim,²⁰ M.J. Kim,⁹ S.B. Kim,²³ S.H. Kim,⁴⁸ T.H. Kim,²⁶ Y.K. Kim,¹⁰ M. Kirby,¹² L. Kirsch,⁴ S. Klimentenko,¹⁴ P. Koehn,³² K. Kondo,⁵⁰ J. Konigsberg,¹⁴ A. Korn,²⁶ A. Korytov,¹⁴ J. Kroll,³⁶ M. Kruse,¹² V. Krutelyov,⁴⁴ S.E. Kuhlmann,² N. Kuznetsova,¹³ A.T. Laasanen,³⁹ S. Lami,⁴¹ S. Lammel,¹³ J. Lancaster,¹² K. Lannon,³² M. Lancaster,²⁵ R. Lander,⁵ A. Lath,⁴³ G. Latino,³⁰ T. LeCompte,² Y. Le,²¹ J. Lee,⁴⁰ S.W. Lee,⁴⁴ N. Leonardo,²⁶ S. Leone,³⁷ J.D. Lewis,¹³ K. Li,⁵² C.S. Lin,¹³ M. Lindgren,⁶ T.M. Liss,²⁰ T. Liu,¹³ D.O. Litvintsev,¹³ N.S. Lockyer,³⁶ A. Loginov,²⁹ M. Loreti,³⁵ D. Lucchesi,³⁵ P. Lukens,¹³ L. Lyons,³⁴ J. Lys,²⁴ R. Madrak,¹⁸ K. Maeshima,¹³ P. Maksimovic,²¹ L. Malferri,³ M. Mangano,³⁷ G. Manca,³⁴ M. Mariotti,³⁵ M. Martin,²¹ A. Martin,⁵² V. Martin,³¹ M. Martinez,¹³ P. Mazzanti,³ K.S. McFarland,⁴⁰ P. McIntyre,⁴⁴ M. Menguzzato,³⁵ A. Menzione,³⁷ P. Merkel,¹³ C. Mesropian,⁴¹ A. Meyer,¹³ T. Miao,¹³ R. Miller,²⁸ J.S. Miller,²⁷ S. Miscetti,¹⁵ G. Mitselmakher,¹⁴ N. Moggi,³ R. Moore,¹³ T. Moulik,³⁹ M. Mulhearn,²⁶ A. Mukherjee,¹³ T. Muller,²² A. Munar,³⁶ P. Murat,¹³ J. Nachtman,¹³ S. Nahn,⁵² I. Nakano,¹⁹ R. Napora,²¹ F. Niell,²⁷ C. Nelson,¹³ T. Nelson,¹³ C. Neu,³² M.S. Neubauer,²⁶ C. Newman-Holmes,¹³ T. Nigmanov,³⁸ L. Nodulman,² S.H. Oh,¹² Y.D. Oh,²³ T. Ohsugi,¹⁹ T. Okusawa,³³ W. Orejudos,²⁴ C. Pagliarone,³⁷ F. Palmonari,³⁷ R. Paoletti,³⁷ V. Papadimitriou,⁴⁵ J. Patrick,¹³ G. Pauletta,⁴⁷ M. Paulini,⁹ T. Pauly,³⁴ C. Paus,²⁶ D. Pellett,⁵ A. Penzo,⁴⁷ T.J. Phillips,¹² G. Piacentino,³⁷ J. Piedra,⁸ K.T. Pitts,²⁰ R. Plunkett,¹³ A. Pomposh,³⁹ L. Pondrom,⁵¹ G. Pope,³⁸ T. Pratt,³⁴ F. Prokoshin,¹¹ A. Pronko,¹⁴ J. Proudfoot,² F. Ptohos,¹⁵ O. Pouchkov,¹¹ G. Punzi,³⁷ J. Rademacker,³⁴ A. Rakitine,²⁶ F. Ratnikov,⁴³ H. Ray,²⁷ A. Reichold,³⁴ P. Renton,³⁴ M. Rescigno,⁴² F. Rimondi,³ L. Ristori,³⁷ W.J. Robertson,¹² T. Rodrigo,⁸ S. Rolli,⁴⁹ L. Rosenson,²⁶ R. Roser,¹³ R. Rossin,³⁵ C. Rott,³⁹ A. Roy,³⁹ A. Ruiz,⁸ D. Ryan,⁴⁹ A. Safonov,⁵ R. St. Denis,¹⁷ W.K. Sakumoto,⁴⁰ D. Saltzberg,⁶ C. Sanchez,³² A. Sansoni,¹⁵ L. Santi,⁴⁷ S. Sarkar,⁴² P. Savard,⁴⁶ A. Savoy-Navarro,¹³ P. Schlabach,¹³ E.E. Schmidt,¹³ M.P. Schmidt,⁵² M. Schmitt,³¹ L. Scodellaro,³⁵ A. Scribano,³⁷ A. Sedov,³⁹ S. Seidel,³⁰ Y. Seiya,⁴⁸ A. Semenov,¹¹ F. Semeria,³ M.D. Shapiro,²⁴ P.F. Shepard,³⁸ T. Shibayama,⁴⁸ M. Shimojima,⁴⁸ M. Shochet,¹⁰ A. Sidoti,³⁵ A. Sill,⁴⁵ P. Sinervo,⁴⁶ A.J. Slaughter,⁵² K. Sliwa,⁴⁹ F.D. Snider,¹³ R. Snihur,²⁵ M. Spezziga,⁴⁵ F. Spinella,³⁷ M. Spiropulu,⁷ L. Spiegel,¹³ A. Stefanini,³⁷ J. Strologas,³⁰ D. Stuart,⁷ A. Sukhanov,¹⁴ K. Sumorok,²⁶ T. Suzuki,⁴⁸ R. Takashima,¹⁹ K. Takikawa,⁴⁸ M. Tanaka,² M. Tecchio,²⁷ R.J. Tesarek,¹³ P.K. Teng,¹ K. Terashi,⁴¹ S. Tether,²⁶ J. Thom,¹³ A.S. Thompson,¹⁷ E. Thomson,³² P. Tipton,⁴⁰ S. Tkaczyk,¹³ D. Toback,⁴⁴ K. Tollefson,²⁸ D. Tonelli,³⁷ M. Tönnemann,²⁸ H. Toyoda,³³ W. Trischuk,⁴⁶ J. Tseng,²⁶ D. Tsybychev,¹⁴ N. Turini,³⁷ F. Ukegawa,⁴⁸ T. Unverhau,¹⁷ T. Vaiciulis,⁴⁰ A. Varganov,²⁷ E. Vataga,³⁷ S. Vejck III,¹³ G. Velez,¹³ G. Veramendi,²⁴ R. Vidal,¹³ I. Vila,⁸ R. Vilar,⁸ I. Volobouev,²⁴ M. von der Mey,⁶ R.G. Wagner,² R.L. Wagner,¹³ W. Wagner,²² Z. Wan,⁴³ C. Wang,¹² M.J. Wang,¹ S.M. Wang,¹⁴ B. Ward,¹⁷ S. Waschke,¹⁷ D. Waters,²⁵ T. Watts,⁴³ M. Weber,²⁴ W.C. Wester III,¹³ B. Whitehouse,⁴⁹ A.B. Wicklund,² E. Wicklund,¹³ H.H. Williams,³⁶ P. Wilson,¹³ B.L. Winer,³² S. Wolbers,¹³ M. Wolter,⁴⁹ S. Worm,⁴³ X. Wu,¹⁶ F. Würthwein,²⁶ U.K. Yang,¹⁰ W. Yao,²⁴ G.P. Yeh,¹³

K. Yi,²¹ J. Yoh,¹³ T. Yoshida,³³ I. Yu,²³ S. Yu,³⁶ J.C. Yun,¹³ L. Zanello,⁴² A. Zanetti,⁴⁷ F. Zetti,²⁴ and S. Zucchelli³

(CDF Collaboration)

- ¹ *Institute of Physics, Academia Sinica, Taipei, Taiwan 11529, Republic of China*
- ² *Argonne National Laboratory, Argonne, Illinois 60439*
- ³ *Istituto Nazionale di Fisica Nucleare, University of Bologna, I-40127 Bologna, Italy*
- ⁴ *Brandeis University, Waltham, Massachusetts 02254*
- ⁵ *University of California at Davis, Davis, California 95616*
- ⁶ *University of California at Los Angeles, Los Angeles, California 90024*
- ⁷ *University of California at Santa Barbara, Santa Barbara, California 93106*
- ⁸ *Instituto de Fisica de Cantabria, CSIC-University of Cantabria, 39005 Santander, Spain*
- ⁹ *Carnegie Mellon University, Pittsburgh, Pennsylvania 15213*
- ¹⁰ *Enrico Fermi Institute, University of Chicago, Chicago, Illinois 60637*
- ¹¹ *Joint Institute for Nuclear Research, RU-141980 Dubna, Russia*
- ¹² *Duke University, Durham, North Carolina 27708*
- ¹³ *Fermi National Accelerator Laboratory, Batavia, Illinois 60510*
- ¹⁴ *University of Florida, Gainesville, Florida 32611*
- ¹⁵ *Laboratori Nazionali di Frascati, Istituto Nazionale di Fisica Nucleare, I-00044 Frascati, Italy*
- ¹⁶ *University of Geneva, CH-1211 Geneva 4, Switzerland*
- ¹⁷ *Glasgow University, Glasgow G12 8QQ, United Kingdom*
- ¹⁸ *Harvard University, Cambridge, Massachusetts 02138*
- ¹⁹ *Hiroshima University, Higashi-Hiroshima 724, Japan*
- ²⁰ *University of Illinois, Urbana, Illinois 61801*
- ²¹ *The Johns Hopkins University, Baltimore, Maryland 21218*
- ²² *Institut für Experimentelle Kernphysik, Universität Karlsruhe, 76128 Karlsruhe, Germany*
- ²³ *Center for High Energy Physics: Kyungpook National University, Taegu 702-701; Seoul National University, Seoul 151-742; and SungKyunKwan University, Suwon 440-746; Korea*
- ²⁴ *Ernest Orlando Lawrence Berkeley National Laboratory, Berkeley, California 94720*
- ²⁵ *University College London, London WC1E 6BT, United Kingdom*
- ²⁶ *Massachusetts Institute of Technology, Cambridge, Massachusetts 02139*
- ²⁷ *University of Michigan, Ann Arbor, Michigan 48109*
- ²⁸ *Michigan State University, East Lansing, Michigan 48824*
- ²⁹ *Institution for Theoretical and Experimental Physics, ITEP, Moscow 117259, Russia*
- ³⁰ *University of New Mexico, Albuquerque, New Mexico 87131*
- ³¹ *Northwestern University, Evanston, Illinois 60208*
- ³² *The Ohio State University, Columbus, Ohio 43210*
- ³³ *Osaka City University, Osaka 588, Japan*
- ³⁴ *University of Oxford, Oxford OX1 3RH, United Kingdom*
- ³⁵ *Universita di Padova, Istituto Nazionale di Fisica Nucleare, Sezione di Padova, I-35131 Padova, Italy*
- ³⁶ *University of Pennsylvania, Philadelphia, Pennsylvania 19104*
- ³⁷ *Istituto Nazionale di Fisica Nucleare, University and Scuola Normale Superiore of Pisa, I-56100 Pisa, Italy*
- ³⁸ *University of Pittsburgh, Pittsburgh, Pennsylvania 15260*
- ³⁹ *Purdue University, West Lafayette, Indiana 47907*
- ⁴⁰ *University of Rochester, Rochester, New York 14627*
- ⁴¹ *Rockefeller University, New York, New York 10021*
- ⁴² *Instituto Nazionale de Fisica Nucleare, Sezione di Roma, University di Roma I, "La Sapienza," I-00185 Roma, Italy*
- ⁴³ *Rutgers University, Piscataway, New Jersey 08855*
- ⁴⁴ *Texas A&M University, College Station, Texas 77843*
- ⁴⁵ *Texas Tech University, Lubbock, Texas 79409*
- ⁴⁶ *Institute of Particle Physics, University of Toronto, Toronto M5S 1A7, Canada*
- ⁴⁷ *Istituto Nazionale di Fisica Nucleare, University of Trieste/ Udine, Italy*
- ⁴⁸ *University of Tsukuba, Tsukuba, Ibaraki 305, Japan*
- ⁴⁹ *Tufts University, Medford, Massachusetts 02155*
- ⁵⁰ *Waseda University, Tokyo 169, Japan*
- ⁵¹ *University of Wisconsin, Madison, Wisconsin 53706*
- ⁵² *Yale University, New Haven, Connecticut 06520*

We report the first model independent measurement of charged particle multiplicities in quark and gluon jets, N_q and N_g , produced at the Tevatron in $p\bar{p}$ collisions with center-of-mass energy 1.8 TeV and recorded by the Collider Detector at Fermilab. The measurements are made for jets with average energies 41 and 53 GeV by counting charged particle tracks in cones with opening angle of $\theta_c=0.28, 0.36, \text{ and } 0.47$ rad around the jet axis. The corresponding jet hardness $Q = E_{jet}\theta_c$ varies in the range from 12 GeV to 25 GeV. At $Q=19$ GeV, the ratio of multiplicities $r = N_g/N_q$ is found to be 1.64 ± 0.17 , where statistical and systematic uncertainties are added in quadrature. The results are in agreement with re-summed perturbative QCD calculations.

We present a new measurement of charged particle multiplicities in quark and gluon jets that is largely independent of theoretical models of fragmentation. This independence is achieved by exploiting the difference in quark and gluon jet content of dijet events and γ +jet events in $p\bar{p}$ collisions. The analysis is carried out in the dijet or γ +jet center-of-mass frame, where the average jet energies are $E_{jet}=41$ and 53 GeV. Multiplicities are measured in restricted cones with $\theta_c=0.28, 0.36, \text{ and } 0.47$ rad, where θ_c is the angle between the jet axis and the cone side. The results are compared to predictions based on perturbative QCD calculations carried out in the framework of the Next-to-Leading Log Approximation (NLLA) [1] and its extensions [3–6], supplemented with the hypothesis of Local Parton-Hadron Duality (LPHD) [7].

In QCD, quarks and gluons have different probabilities to emit gluons, and it is therefore expected that jets produced by quarks and gluons will show a difference in their average hadron multiplicity. The NLLA+LPHD approach views jet fragmentation as a predominantly perturbative QCD process. The NLLA calculations give the average number of partons, $N_{partons}(Y)$, in a small cone with opening angle θ_c around the jet direction as a function of $Y=\ln Q/Q_{eff}$, where $Q=E_{jet}\theta_c$ is the jet hardness and Q_{eff} is the lowest allowed transverse momentum of partons with respect to the jet direction. The LPHD hypothesis assumes that hadronization occurs locally at the end of the parton shower development so that the properties of hadrons are closely related to those of the partons. For instance, the hadron and parton multiplicities are assumed to be related via a constant factor K_{LPHD} , i.e., $N_{hadrons}=K_{LPHD}N_{partons}$, which is independent of the jet energy and of whether the jet originates from a quark or a gluon. In this approach, the ratio of hadron multiplicities in gluon and quark jets, $r=N_g/N_q$, is the same as the ratio of partons. Various calculations for the latter ratio are presented in Fig. 1.

Measurements of multiplicity differences between quark and gluon jets have a long history, most of which comes from e^+e^- colliders. The earliest measurements of the ratio r were consistent with 1 ([8,9] and references therein). Over the 10-year LEP era, the reported values varied from $r\simeq 1.1$ to $r\simeq 1.5$ [8]. For purposes of comparison, we show in Fig. 1 recent CLEO [10] and OPAL [11] data points. These are believed to be model-independent and the least biased by jet-finding algorithms (see [8]).

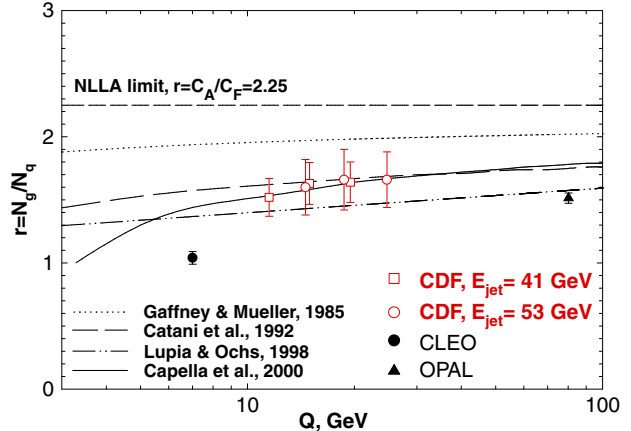


FIG. 1. The ratio of charged particle multiplicities in gluon and quark jets as a function of jet hardness Q , which is $Q=E_{jet}\theta_c$ for CDF data and $Q=E_{c.m.}=2E_{jet}$ for e^+e^- data [10,11]. CDF results (this paper) are obtained for cone sizes $\theta_c=0.28, 0.36, \text{ and } 0.47$ rad. The NLLA curves [3–6] are calculated using $Q_{eff}=230$ MeV [12]. The asymptotic value ($Q\rightarrow\infty$, [2]) of r is simply the ratio of the gluon and quark color charges, $C_A=3$ and $C_F=4/3$, respectively.

The range of e^+e^- results motivates an independent measurement of r in a different environment such as $p\bar{p}$ collisions. The charged particle multiplicities in gluon and quark jets, N_g and N_q respectively, as well as their ratio r , can be extracted by comparing the multiplicities in two data samples with very different fractions of gluon jets; thus we do not have to discriminate between quark and gluon jets when selecting events. Two such samples used in the analysis are dijet and γ +jet events, for which:

$$N_{jj} = f_g^{jj} N_g + (1 - f_g^{jj}) N_q, \quad (1)$$

$$N_{\gamma j} = f_g^{\gamma j} N_g + (1 - f_g^{\gamma j}) N_q, \quad (2)$$

where N_{jj} and $N_{\gamma j}$ are the average charged particle multiplicities per jet in, respectively, dijet and γ +jet events, and f_g^{jj} and $f_g^{\gamma j}$ are fractions of gluon jets in dijet and γ +jet events. To take into account the contamination of γ +jet events by fake photons, Equation (2) must be modified as follows:

$$N_{\gamma j} = \delta_\gamma (f_g^{\gamma j} N_g + (1 - f_g^{\gamma j}) N_q) + (1 - \delta_\gamma) N_{fj}, \quad (3)$$

where δ_γ is the fraction of real photons among the photon

candidates, and N_{fj} is the multiplicity in the jet opposite to the fake photon.

The current results are based on events produced in $p\bar{p}$ collisions with center-of-mass energy $\sqrt{s}=1.8$ TeV and recorded by the Collider Detector at Fermilab (CDF) during the 1993-1995 run period. The total integrated luminosity is 95 ± 7 pb $^{-1}$. The CDF detector is described in [13] and references therein. Here, we briefly describe only those elements of the detector that are relevant to this analysis. The CDF coordinate system and basic variables are defined in [14].

The z -positions of all interaction vertices along the beam line are measured by the vertex detector, which is made of time-projection drift chambers. The Silicon Vertex Detector (SVX) is used to determine the (x, y) -positions of interaction vertices. The Central Tracking Chamber (CTC) consists of open-cell drift chambers designed for measuring charged particle trajectories. Charged particle momentum measurement is based on the trajectory's curvature in the solenoidal magnetic field of 1.4 T. The CTC fully covers the region $|\eta|<1.0$ and gives momentum resolution of $\delta p_T/p_T^2 \leq 0.002$ (GeV/ c) $^{-1}$.

The energy and direction of photons and jets are measured in the central lead-scintillator electromagnetic and iron-scintillator hadronic calorimeters. The calorimeter segmentation is 15° in ϕ and 0.1 in η . For our data sample, the jet energy resolution is $\sim 13\%$ and the photon energy resolution is $\sim 3\%$.

The measurement of the fraction of real photons among the photon candidates is based on evaluating the γ -conversion probability in the central preshower multiwire proportional chambers located in front of the electromagnetic calorimeter. It also uses the transverse profile of the electromagnetic shower, which is measured by means of the shower maximum detector placed inside the electromagnetic calorimeter at the depth of the electromagnetic shower maximum.

In this measurement, the jets are defined by a cone algorithm with cone radius $R=\sqrt{(\Delta\phi)^2 + (\Delta\eta)^2}=0.7$; full details can be found in [15]. Corrections are applied to the raw jet energy in the cone: to compensate for the non-linearity and non-uniformity of the energy response of the calorimeter; to subtract the energy deposited in the jet cone by sources other than the initial parton (underlying event, multiple interactions etc.); and to add the energy radiated by the initial parton out of the jet cone (out-of-cone correction). Both jet direction and energy are derived from the calorimeter information alone. The overall uncertainty on the jet energy scale is 5%. To evaluate possible biases that might originate from the particular choice of jet-finding algorithm, we studied the properties of jets reconstructed by using smaller ($R=0.4$) and larger ($R=1.0$) cones. Variations are taken as an estimate of the corresponding systematic uncertainty.

The dijet sample is accumulated by using the inclusive jet trigger with E_T threshold 20 GeV. The trigger is pre-scaled by 1000. The γ +jet sample is collected using

the inclusive photon triggers with thresholds of 23 and 50 GeV on E_T . To reduce the contamination from fake photons in the lower energy γ +jet sample, the 23 GeV trigger requires photon isolation, i.e. extra transverse energy (other than candidate energy) in neighboring calorimeter towers around the candidate has to be less than 4 GeV.

The dijet events are required to have two jets balanced in P_T : $|\vec{P}_{T_1} + \vec{P}_{T_2}|/(P_{T_1} + P_{T_2}) < 0.15$ ($\sim 2\sigma_{P_T}$). Only events with both jets in the central region of the detector ($|\eta_{1,2}| < 0.9$) are retained to ensure efficient track reconstruction. The events are required to have no more than two well-reconstructed primary vertices. For events with two primary interactions, all tracks are associated with vertices by their proximity. The separation between vertices along the beam line is required to be larger than 12 cm ($\sim 12\sigma_z$ for tracks) to allow for unambiguous assignment of tracks. The vertex that has the largest ΣP_T of tracks from cones with $R=0.7$ around the jet directions is taken to be the one associated with the hard collision.

The γ +jet events must pass exactly the same cuts (treating the photon as one of two jets) and satisfy specific photon identification requirements. A cut on the fraction of energy of the photon candidate observed in the hadronic calorimeter, $E_{HA}/E_{total} < 0.125$, is applied to suppress hadronic background. The selected events are required to have exactly one photon candidate with $E_T > 20$ GeV and no more than 1 GeV of extra transverse energy in a cone of $R=0.4$ around the photon candidate. The last requirement is the photon isolation cut. To remove electrons and further suppress QCD background, events are rejected if they have tracks pointing to the photon candidate cluster. The electromagnetic transverse shower profile measured by the shower maximum detector has to be consistent with that of a single photon.

Applying the same energy balance cut to dijet and γ +jet events could lead to a small difference between jets from these samples. To evaluate this effect we use a tighter cut (motivated by Monte Carlo studies) for γ +jet events: $|\vec{P}_{T_1} + \vec{P}_{T_2}|/(P_{T_1} + P_{T_2}) < 0.125$. Variations in the results are found to be small and are conservatively taken as estimates of the associated systematic uncertainty. The results of the analysis also do not show any significant dependence on the number of primary vertices or on the photon isolation cut.

The selected events are then subdivided into two bins according to invariant mass, which is defined as $M = \sqrt{(E_1 + E_2)^2/c^4 - (\vec{P}_1 + \vec{P}_2)^2/c^2}$, where E_i and \vec{P}_i are the jet or photon energy and momentum and jets are treated as massless objects. The bins have width $\Delta \ln M = 0.3$, which is chosen to be greater than the dijet mass spread due to calorimeter resolution, $\frac{\delta M}{M} \simeq 10\%$. In the lower bin (72-94 GeV/ c^2), our sample consists of 3602 dijet and 2526 γ +jet events with an average invariant mass of 82 GeV/ c^2 . The other bin (94-120 GeV/ c^2) has 1768 dijet and 910 γ +jet events with an average invariant mass of 105 GeV/ c^2 . The results of the analysis are corrected for a small difference (< 1 GeV) in the

average invariant mass of dijet and γ +jet events. This difference is an effect of the jet trigger threshold. The small correction of $<1\%$ is taken as an estimate of the corresponding systematic uncertainty.

The analysis is carried out in the dijet (or γ +jet) center of mass frame, so that $E_{jet}=Mc^2/2$. Multiplicities are measured for tracks in cones of size $\theta_c=0.28, 0.36,$ and 0.47 rad.

The fractions of gluon jets in dijet events, f_g^{jj} , and pure γ -jet events, f_γ^j , are determined from Herwig 5.6 [16] and Pythia 6.115 [17] Monte Carlo generators with parton distribution function (PDF) sets [18] CTEQ4M, CTEQ4A2, and CTEQ4A4. Typical values are found to be $f_g^{jj}\sim 60\%$ and $f_\gamma^j\sim 20\%$. The systematic uncertainty of $\sim 2\%$ on these fractions is estimated from the differences observed with the two Monte Carlo generators and three different PDF sets.

To estimate the fraction δ_γ of real photons among photon candidates, we use a procedure described in [19]. The fraction is found to be $75\pm 7\%$ and $90\pm 10\%$ for events with $E_{jet}=41$ and 53 GeV, respectively. The method is based on measuring the fraction of events with conversions in the preshower detector. Fake photons are mostly energetic π^0 's or η 's from one of the jets in a dijet event. Therefore fakes, being two almost collinear photons, have a higher conversion probability than does a single prompt photon. The uncertainty in the fraction of real photons, δ_γ , is taken into account in evaluating the corresponding systematic uncertainty in our measurements.

To measure the multiplicity of charged particles associated with jets in dijet and γ +jet events (N_{jj} and $N_{\gamma j}$), we count 3-dimensionally reconstructed tracks and use vertex cuts on impact parameter, d , and $\Delta z=|z_{track}-z_{vertex}|$ (see [20] for details). These cuts exclude tracks originating from secondary interactions in the same bunch crossing, γ -conversions, K_S^0 and Λ decays, cosmic rays, and other backgrounds. The vertex cuts are varied to study the systematic uncertainties associated with them. After applying all the vertex cuts, there still remains a small number of tracks due to γ -conversions and K_S^0 or Λ decays, which is estimated using Herwig 5.6 and the CDF detector simulation package. The corrections are typically $\sim 3.5\%$ (γ -conversions) and $\sim 4\%$ (decays) of the measured multiplicity. The systematic uncertainties assigned to these corrections are equal to their magnitudes.

The measured multiplicities are corrected for track reconstruction inefficiency. The inefficiency was studied by embedding tracks found in one jet into the opposite jet at the CTC hit level and re-doing the full track reconstruction (see [12] for details). Corrections obtained this way take into account the efficiency dependence on jet energy, particle momentum, and particle angle with respect to the jet axis. The size of these corrections on average multiplicities is 6-8%, depending on jet energy and cone size θ_c . The associated systematic uncertainties are estimated by varying the tightness of the criteria

used in matching the parameters of the embedded tracks to those of the re-reconstructed tracks.

Tracks coming from the underlying event and multiple interactions in the same bunch crossing (with unresolved z -vertices) are subtracted on average using complementary cones. A pair of complementary cones is defined such that their axis is in the plane normal to the dijet direction and at the same polar angle as the dijet axis. These cones are assumed to collect statistically the same uncorrelated background as the cones around the jets. This correction varies with cone size from 0.2 to 0.5 tracks per cone.

We also apply a correction for losses of very low P_T tracks due to bending in the magnetic field of the solenoid. The efficiency for reconstructing tracks with $P_T<200$ MeV/ c is almost zero. The correction obtained from the Herwig simulation is typically less than 2%. The systematic uncertainty on this correction is taken to be the correction itself.

The charged particle multiplicity in the jet opposite to the fake photon, N_{fj} , is estimated based on Monte Carlo studies of (fake γ)+jet events. It is found that fake photons, on average, carry only $\sim 90\%$ of the original jet energy (mainly because fake photons can be accompanied by other particles from the original jet), which results in mis-measurement of the event invariant mass by $\sim 5\%$. Such events have true invariant mass higher than it would appear in the analysis and, consequently, the jets have higher multiplicities. We estimate N_{fj} by considering the ratio $\alpha=N_{fj}/N_{jj}$ using Herwig and Pythia, and by taking the dijet data sample and shifting the energy of one of the jets down by 10% to mimic a fake photon. The average of all three methods gives $\alpha\sim 1.04$. The spread in values of α ($\pm 1.3\%$) is used to estimate the corresponding systematic uncertainty.

The major sources of systematic uncertainty in the measurement of charged particle multiplicity in quark and gluon jets are as follows: background track removal, 7-10%; jet-finding algorithm, 1-7%; jet energy measurements, 2-5%; and photon sample purity, 1-4%. The major sources of systematic uncertainty in the measurement of the ratio, r , are as follows: jet energy measurements, 4-9%; photon sample purity, 4-6%; track cuts and corrections, 3-6%; and energy balance, 1-5%. The remaining sources of systematic uncertainties, all combined, total to no more than $\sim 4\%$. The individual systematic uncertainties for results with different jet hardness are strongly correlated.

The average multiplicities of charged particles in gluon and quark jets, N_g and N_q , for two different jet energies and three opening angles, as well as their ratio r , are summarized in Table I and presented in Fig. 1 and Fig. 2. The ratio agrees well with re-summed perturbative QCD calculations, $1.4\leq r\leq 1.8$ [3-6], and is consistent with recent results from OPAL, $r\sim 1.5$ [11]. The ratio is also in good agreement with the previous CDF model-dependent measurement, $r=1.7\pm 0.3$ [21]. From Fig. 1, one can see that the ratio r tends to increase with energy scale. This

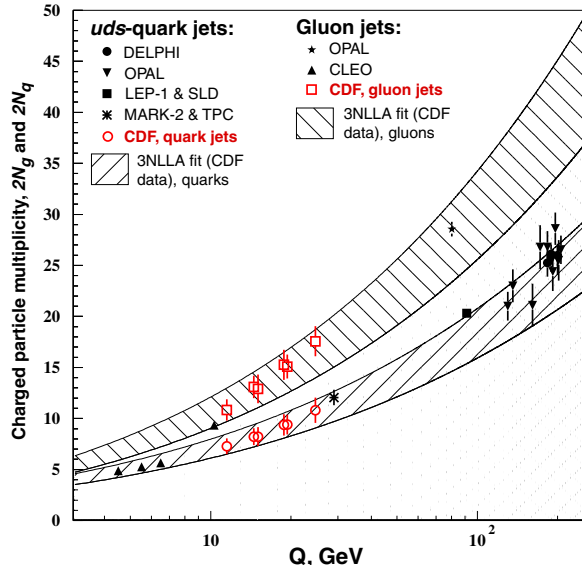


FIG. 2. Average charged particle multiplicities in gluon and quark jets as a function of jet hardness Q , which is $Q=E_{jet}\theta_c$ for CDF data and $Q=E_{c.m.}=2E_{jet}$ for e^+e^- data. For the purpose of comparison to the e^+e^- measurements [10,11,22], CDF results on this plot include charged particles from K_S^0 and Λ decays and are multiplied by two. The fits to CDF data are obtained by using the recent NLLA expressions from Ref. [5] with normalization constant as the only free parameter (the other parameter Q_{eff} is set to 230 MeV [12]). The width of the bands corresponds to the uncertainty in the overall normalization.

trend is statistically significant, because the uncertainties are strongly correlated. At jet energy $E_{jet}=41$ GeV and opening angles $\theta_c=0.28$ and 0.47 rad ($Q=11.5$ GeV and 19.2 GeV), we find $\Delta r=r(19.2 \text{ GeV})-r(11.5 \text{ GeV})=0.12\pm 0.02(\text{stat})\pm 0.05(\text{syst})$ ($\sim 2\sigma$ significance level). The average charged particle multiplicities follow the predicted evolution with jet energy and opening angle as a function of $Q=E_{jet}\theta_c$. To fit our data, we use the recent NLLA expressions from ref. [5] with normalization constant as the only free parameter (the other parameter, Q_{eff} , is set to 230 MeV [12]). The fits for gluon and quark jet data points are independent. One can see that the e^+e^- results, except for CLEO data points around 5-7 GeV, fall within the fit bands.

We compare Pythia 6.115 and Herwig 5.6 predictions with the results of this analysis. For the range of jet hardness, Q , used in our analysis, both Herwig and Pythia predict the ratio r to be 1.2-1.4. Pythia systematically gives $\sim 3-4\%$ higher multiplicities than does Herwig. Both Monte Carlo generators are found to reproduce the gluon jet multiplicities fairly well, but they systematically overestimate the multiplicities in quark jets by as much as 30% (hence, the ratio in Monte Carlo data is lower). The discrepancy is at the level of $\sim 2\sigma_{syst}$.

In summary, we have measured the multiplicities in gluon and quark jets and their ratio, $r=N_g/N_q$, for average jet energies $E_{jet}=41$ and 53 GeV and opening angles

$\theta_c=0.28, 0.36,$ and 0.47 rad. The results are found to agree with re-summed NLLA calculations and are consistent with recent e^+e^- measurements [10,11,22].

We are grateful to Yu. Dokshitzer, I. Dremin, V. Khoze, A.H. Mueller, V. Nechitailo, W. Ochs, R. Peschanski, and B. Webber for a number of very fruitful discussions. We thank the Fermilab staff and the technical staffs of the participating institutions for their vital contributions. This work was supported by the U.S. Department of Energy and National Science Foundation; the Italian Istituto Nazionale di Fisica Nucleare; the Ministry of Education, Culture, Sports, Science and Technology of Japan; the Natural Sciences and Engineering Research Council of Canada; the National Science Council of the Republic of China; the Swiss National Science Foundation; the A.P. Sloan Foundation; the Bundesministerium fuer Bildung und Forschung, Germany; the Korean Science and Engineering Foundation and the Korean Research Foundation; the Particle Physics and Astronomy Research Council and the Royal Society, UK; the Russian Foundation for Basic Research; the Comision Interministerial de Ciencia y Tecnologia, Spain; in part by the European Community's Human Potential Programme under contract HPRN-CT-20002, Probe for New Physics; and by the Research Fund of Istanbul University Project No. 1755/21122001.

-
- [1] Yu. Dokshitzer, V. Khoze, A. Mueller, and S. Troyan, *Basics of Perturbative QCD*, edited by J. Tran Thanh Van (Editions Frontières, Gif-sur-Yvette, 1991).
 - [2] S.J. Brodsky and J.F. Gunion, Phys. Rev. Lett. **37**, 402 (1976); K. Konishi, A. Ukawa, and G. Veneziano, Nucl. Phys. B **157**, 45 (1979).
 - [3] J.B. Gaffney and A.H. Mueller, Nucl. Phys. B **250**, 109 (1985).
 - [4] S. Catani *et al.*, Nucl. Phys. B **377**, 445 (1992).
 - [5] A. Capella *et al.*, Phys. Rev. D **61**, 074009 (2000).
 - [6] S. Lupia and W. Ochs, Phys. Lett. B **418**, 214 (1998).
 - [7] Ya.I. Azimov, Yu. Dokshitzer, V. Khoze, and S. Troyan, Z. Phys. C **27**, 65 (1985); **31**, 213 (1986).
 - [8] I.M. Dremin and J.W. Gary, Phys. Rept. **349**, 301 (2001).
 - [9] V. Khoze *et al.*, in *At the frontier of particle physics: Handbook of QCD*, vol.2, p.1101, edited by M.A. Shifman (World Scientific, 2001).
 - [10] M.S. Alam *et al.*, Phys. Rev. D **56**, 17 (1997).
 - [11] G. Abbiendi *et al.*, Eur. Phys. J. C **11**, 217 (1999).
 - [12] D. Acosta *et al.*, Phys. Rev. D **68**, 012003 (2003).
 - [13] F. Abe *et al.*, Nucl. Instrum. Methods Phys. Res. A **271**, 387 (1988).
 - [14] The CDF coordinate system is defined with respect to the proton beam direction (+z direction). The azimuthal angle ϕ is measured around the beam axis. The pseudorapidity $\eta=-\ln(\tan(\theta/2))$ is used in place of the polar angle

- θ . The jet transverse energy is defined as $E_T = E \sin \theta$.
- [15] F. Abe *et al.*, Phys. Rev. D **45**, 1448 (1992).
- [16] G. Marchesini *et al.*, Comput. Phys. Commun. **67**, 465 (1992).
- [17] T. Sjöstrand *et al.*, Comput. Phys. Commun. **135**, 238 (2001).
- [18] H.L. Lai *et al.*, Phys. Rev. D **55**, 1280 (1997).
- [19] D. Acosta *et al.*, Phys. Rev. D **65**, 112003 (2002).
- [20] The impact parameter, d , is the shortest transverse distance between the interaction point and the particle trajectory. The Δz is the difference between the z position of the track at the point of its closest approach to the beam line and the position of the primary vertex. We use

- the same cuts on d and Δz as in [12] and [21].
- [21] T. Affolder *et al.*, Phys. Rev. Lett. **87**, 211804 (2001).
- [22] Mark II Collab.: P.C. Rowson *et al.*, Phys. Rev. Lett. **54**, 2580 (1985); TPC Collab.: H. Aihara *et al.*, Phys. Lett. B **184**, 299 (1987); CLEO Collab.: M.S. Alam *et al.*, Phys. Rev. D **46**, 4822 (1992); SLD Collab.: K. Abe *et al.*, Phys. Lett. B **386**, 475 (1996); DELPHI Collab.: P. Abreu *et al.*, Eur. Phys. J. C **6**, 19 (1999); Phys. Lett. B **479**, 118 (2000); Erratum *ibid.* **492**, 398 (2000); OPAL Collab.: K. Ackerstaff *et al.*, Eur. Phys. J. C **1**, 479 (1998); G. Abbiendi *et al.*, Phys. Lett. B **550**, 33 (2002).

TABLE I. Charged particle multiplicities in small cones around gluon and quark jet directions and their ratio: N_g , N_q , and $r = N_g/N_q$, respectively. Multiplicities do not include charged particles from K_S^0 and Λ decays.

E_{jet}	41 GeV			52.5 GeV			
	cone size, θ_c	0.28 rad	0.36 rad	0.47 rad	0.28 rad	0.36 rad	0.47 rad
$Q = E_{jet}\theta_c$		11.5 GeV	14.7 GeV	19.2 GeV	14.7 GeV	18.9 GeV	24.7 GeV
N_g		4.98±0.07±0.52	6.02±0.08±0.55	6.94±0.08±0.58	5.94±0.12±0.69	7.02±0.13±0.72	8.08±0.14±0.72
N_q		3.28±0.11±0.37	3.70±0.11±0.40	4.23±0.12±0.47	3.70±0.17±0.43	4.22±0.18±0.49	4.86±0.19±0.57
$r = \frac{N_g}{N_q}$		1.52±0.08±0.13	1.63±0.09±0.14	1.64±0.09±0.14	1.60±0.12±0.19	1.66±0.13±0.20	1.66±0.13±0.18